Analysis of Microstructural Damage to Aluminum Electrodes Due to Ohmic Heating in the Pasteurization Process of Honey Using the Edge Detection Method

Elvianto Dwi Hartono [1], Puspita Pratama [1], Ery Sadewa Yudha [2], Supangat [3]
[1] Department of Robotics & Artificial Intelligence, University of 17 August 1945 Surabaya
[1,2] Department of Computer Science, University of 17 August 1945 Surabaya
Jl. Semolowaru No.45, Menur Pumpungan, Sukolilo District, Surabaya, East Java, INDONESIA
Email:, puspitapratama1307@gmail.com ***Corresponding Author*** : elvianto.evh@untag-sby.ac.id

Food safety and the effectiveness of pasteurization are key concerns in the food industry, particularly for high-value products like honey. This study evaluates the microstructural damage of aluminum electrodes during honey pasteurization using ohmic heating at frequencies of 50 Hz, 300 Hz, 1 kHz, and 3 kHz. One of the challenges is electrode degradation caused by electrochemical reactions that may contaminate the product. To detect degradation, two hybrid edge detection methods (Canny-Sobel) and HED were compared using 16 electrode images, with evaluation metrics including MSE, PSNR, SSIM, FSIM, Entropy, and metal contamination analysis via ICP-OES. The results show that the deep learning CNN-based HED provides more accurate and detailed detection, with the highest image changes occurring at a frequency of 3 kHz (left electrode) with metric results: MSE 108.557, PSNR 27.774 dB, SSIM 0.824, FSIM 0.001, and Entropy 2.282. These findings highlight the potential of deep learning in automated monitoring systems for electrode degradation to enhance the quality and safety of food products sustainably.

Keywords: Edge Detection, Aluminum Electrode, Product Safety, Ohmic Heating, Honey Pasteurization

I. INTRODUCTION

Food processing technology continues to advance with a focus on improving food safety, shelf life, and nutrient preservation. One significant innovation is ohmic heating, which offers energy efficiency, precise temperature control, and the ability to maintain product quality. This technology is highly relevant for high-value products like honey, which require specialized pasteurization processes to preserve bioactive compounds. However, despite its effectiveness, ohmic heating still faces technical challenges that need to be addressed (Sumarlin *et al.*, 2022).

One of the main challenges in ohmic heating is aluminum electrode corrosion caused by electrochemical reactions, which can contaminate the final product and reduce process effectiveness. Therefore, an accurate electrode condition monitoring system is required. Digital image processing technology offers a suitable solution through edge detection methods such as Canny and Sobel. Although these algorithms have been widely applied in medical and general object fields, their application in detecting electrode microstructure degradation in food processing remains limited, particularly regarding metal contamination (Mercali *et al.*, 2013).

This study aims to analyze the microstructural damage of aluminum electrodes during honey pasteurization using ohmic heating at different frequencies. Two edge detection approaches were employed: the combination of Canny-Sobel and Holistically-Nested Edge Detection (HED) based on deep learning. The detection results were evaluated using metrics such as MSE, PSNR, SSIM, FSIM, and Entropy, and then compared with metal contamination levels using ICP-OES testing. This study is expected to serve as a foundation for the development of a non-destructive monitoring system to ensure the safety and quality of food products in a sustainable manner.

II. LITERATURE REVIEW

A. Honey (Trigona Sp)

West Nusa Tenggara (NTB) is known as one of the leading honey-producing regions in Indonesia, particularly honey from stingless bees of the *Trigona sp. species.* This honey has unique characteristics such as color, taste, viscosity, and nutritional content that differ from other types of honey. Its nutritional content is also very high because Trigona bees can collect nectar from flowers that are difficult to reach (Syahruddin *et al.*, 2022).

In ohmic heating, honey functions as a conductive medium, where water content and sugar levels influence efficiency and interaction with electrodes. The chemical reactions that occur can damage diastase enzymes and reduce honey quality, making temperature control and heating duration critical to preserving its benefits.

Fig. 1 *Trigona Sp* Honeybee

B. Aluminum Metal

Aluminum is a lightweight and conductive metal resistant to corrosion due to its oxide layer. However, in ohmic heating, electrochemical reactions with honey can

cause corrosion, reduce efficiency, and contaminate the product. Therefore, selecting the appropriate electrode is crucial for maintaining honey quality and safety. The following aluminum metals are used during the ohmic heating process:

Fig. 2 Aluminum Metal Electrode

C. Ohmic Heating

Ohmic heating is a pasteurization method that uses alternating current (AC) electricity flowing through food materials to generate heat directly. The food serves as a resistor, and heating occurs when current flows through the electrodes from the power source to the reactor. The heating rate is greatly influenced by the electrical conductivity of the material, which depends on ion concentration, temperature, moisture content, pH, and ion composition. For each type of material, electrical conductivity can be calculated using the following equation:

$$\sigma = \frac{L}{A} \times \frac{I}{V} \quad (1)$$

Where:

- σ : Electrical Conductivity
- A : Cross-sectional area (m²)
- L : Distance between electrodes (m)
- I : Current passing through the material
- V : Voltage (*Volt*)

Ohmic heating is based on the fundamentals of Ohm's law, which describes the relationship between voltage (V), electric current (I), and resistance (R) in an electrical circuit. This relationship can be expressed in the equation:

$$I = V/R \quad (2)$$

Where

- V : Applied voltage (*Volts*)
- I : Current intensity (Amperes)
- R : Electrical Resistance of the Conductor (Ohms)

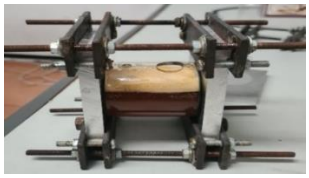

Fig. 3 *Prototype* Ohmic *Treatment Chamber*

D. Digital Image

An image is a visual representation on a two-dimensional surface. A digital image can be defined as a function of intensity that depends on two variables, f(x,y), where x and y are spatial coordinates and the value of the function at each point (x,y) is the gray level of the image at that point. A digital image is represented by a matrix consisting of M columns and N rows, where each intersection between a column and a row is called a pixel (pixel = picture element), which is the smallest element of an image (Kurniawati and Kusumawardhani, 2017).

E. Digital Image Processing

Image processing is the science that studies matters related to improving the quality of an image (contrast enhancement, color transformation, restoration), image transformation (rotation, translation, scaling, geometric transformations), performing optimal image feature extraction for analysis purposes, extracting information or describing objects contained in an image, as well as compressing or reducing data for storage, data transmission, and data processing time (Munantri, Sofyan, and Florestiyanto, 2020).

F. Edge Detection

Edge detection is a process that produces the edges of image objects, which aims to mark the parts that become image details and to improve blurred image details caused by errors or the effects of the image acquisition process (Herawati and Kardian, 2018). A point (x, y) is defined as an edge in an image if it has a high pixel value difference from its neighbors.

In image classification, edge detection is crucial before image segmentation. Object boundaries in an image can be identified through differences in grayscale levels. Edge detection is used to reconstruct blurred image details caused by image distribution effects. Edge detection can also transform a 2D image into a curve.

F.1 Canny Edge Detection

The Canny edge detection method was proposed by John Canny in 1986 and is known as one of the most optimal edge detection algorithms. This method involves several steps, including Gaussian filtering, gradient detection, non-maximum suppression, and hysteresis. The following are the steps in performing Canny edge detection:

1. Image Smoothing
   Filtering is performed on the image to remove noise, using simple Gaussian filtering, with the condition that the filtering volume is significantly smaller than the image size.
2. Calculating Intensity Gradients
   After the image is smoothed, the next step is to calculate the edge strength using a Gaussian operator. The image gradient is calculated using the formula:

$$|G| = \sqrt{G_x^2 + G_y^2} \quad (3)$$

3. Calculating Edge Direction
   The edge direction is calculated using the formula:

$$\theta = \tan^{-1}\left(\frac{G_y}{G_x}\right) \quad (4)$$

4. Non-Maximum Suppression
   Non-maximum suppression is performed after gradient orientation is obtained, with the aim of sharpening the gradient image. This process removes pixels that are not local maxima along the gradient direction, so that blurred areas in the image become sharper and the edges become clearer.
5. Hysteresis Thresholding
   This process smooths lines on the image surface using two thresholds, T1 and T2. Pixels whose values exceed T1 are considered edges, and connected pixels whose values are above T2 are also classified as edges.

The Canny edge detection process is performed by reading each pixel in the image, starting from the top-left corner (northeast) and moving to the bottom-right corner (southwest). Therefore, to support the edge detection process, the Gx and Gy gradients are each calculated using a 3x3 Canny operator matrix.

-1	0	1
-2	0	2
-1	0	1

Gx

1	2	1
0	0	0
-1	-2	-1

Gy

Fig. 4 3x3 *Canny* Operator Matrix

F.2 Sobel Edge Detection

Sobel edge detection is a technique in digital image analysis used to identify objects by detecting significant changes in pixel intensity. This method is an extension of the Roberts method, utilizing a High Pass Filter with a zero element to reduce noise before the detection process. Sobel employs two 3x3 convolution matrices to calculate horizontal (Gx) and vertical (Gy) gradients, which measure pixel intensity differences around the central point in horizontal and vertical directions, resulting in clearer and more accurate edge detection.

1	2	1
0	0	0
-1	-2	-1

-1	0	1
-2	0	2
-1	0	1

Fig. 5 3x3 *Sobel* Operator Matrix

F.3 Holistically Nested Edge Detection (HED)

Holistically Nested Edge Detection (HED) is a deep learning-based edge detection method that combines *a Full Convolutional Network* (FCN) with end-to-end deep supervision. HED collects information from various levels of the network (multi-scale and multi-level) to analyze images comprehensively, both locally and globally. Each layer of the network produces partial edge predictions, which are then combined using specific weights to form a more accurate final edge detection.

G. MSE (Mean Square Error)

Mean Squared Error (MSE) determines the level of difference between the mean and median. The MSE value is obtained from the difference between the first and second images with the same pixel positions. An increase in MSE indicates a significant difference between the initial and final images. MSE estimation uses the equation. The values of m and n represent the length and width of the image. I(i,j) is the initial image, and K(i,j) is the edge detection result image (Mustafid and 'Uyun, 2017).

$$MSE = \frac{1}{mn}\sum_{i=0}^{m-1}\sum_{j-0}^{n-1}[(i,j) - K(i,j)^2 \qquad (5$$

During the image reconstruction, restoration, and compression processes, the MSE will decrease. However, in image edge detection, if the MSE reaches a high value, this indicates that there are many detected image edges and sharper image edge signals can be identified.

H. Peak Signal to Noise Ratio (PSNR)

Peak Signal to Noise Ratio (PSNR) is a method for measuring image quality by comparing the maximum signal value to the level of disturbing noise. PSNR is expressed in decibels (dB), and the higher the value, the better the image quality. It is commonly used to evaluate the results of image compression or reconstruction. The maximum value (R) for an 8-bit image is typically 255. PSNR calculations require precision to ensure accurate results.

$$PSNR = 10\,log_{10}\left(\frac{R^2}{MSE}\right) \qquad (6)$$

I. SSIM (Structural Similarity Index Measure)

SSIM is a method used to determine the similarity between two images with good consistency with the Human Visual System (HVS). The SSIM algorithm compares the structural features of an image, using structural similarity to determine its quality (Wulandari, 2017). SSIM divides the comparison of two images into three main parts that represent different aspects of human visual perception, namely:

- Luminance= : Measures the similarity of the average light intensity between two images.
- Contrast= : Measures the similarity of intensity variation or contrast distribution between the two images.
- Structure= : Measures the similarity of structural patterns or spatial relationships between pixels in the two images.

These three components are then mathematically combined to produce an overall similarity index. Mathematically, the equation for the SSIM index between signals x and y is defined as:

$$SSIM = [I\,(x,y)]^{\alpha} \times [C\,(x,y)]^{\beta} \times [S\,(x,y)]^{\gamma} \qquad (7)$$

J. FSIM (Feature Similarity Index Metrics)

FSIM is an image quality assessment metric that measures the similarity of low-level features between a reference image and a test image based on human visual system (HVS) perception. FSIM has two main features, namely *Phase Congruency* (PC) and *Gradient Magnitude* (GM) (Wulandari, 2017). GM of an image is defined as:

$$G = \sqrt{{G_x}^2 + {G_y}^2} \quad (8)$$

Where G_x (x) is the vertical gradient of the image and G_y (y) is the horizontal gradient of the image. The purpose is to separate the feature similarity measurement between the original image f_1 (x) and the test image $f_2(x)$.

K. Entropy

Entropy indicates the complexity of an image. The more complex an image, the higher its entropy level. The following is the entropy calculation:

$$Entropy = \sum_{i=0}^{N-1}\sum_{j=0}^{N-1} p_{(i,j)} log\left(p_{(i,j)}\right) \quad (9)$$

Where:

- μi = average value of row elements
- μj = average value of column elements
- σi = standard deviation of the row elements in the matrix p (i,j)
- σj = standard deviation of the elements in the columns of matrix p (i,j)

L. MATLAB (Matrix Laboratory)

MATLAB is a matrix-based numerical computing software for data analysis and mathematical calculations. Equipped with built-in functions and a graphical interface, MATLAB supports interactive visualization and GUI-based application development. Users can also add features as needed.

M.PYTHON

Python is a popular programming language created by Guido van Rossum in the 1990s. Known for its simplicity and ease of use, Python is widely used in industry and education to create desktop, web, and mobile applications. Its popularity makes it the top choice for IT students. Although easy to use, programming with Python still requires a good understanding of algorithms.

III. RESEARCH METHOD

A. Research Location and Time

This research was conducted at the PT. Best Energy System ( ) located at , in the Plaza Segi 8 Complex, Block C No. 841, Jl. Pattimura, Surabaya, East Java, Indonesia. The research activities took place from January to April 2025, encompassing the proposal development stage through to the processing and compilation of research results.

B. Research Materials and Equipment

The equipment used in this research includes a laptop, microscope, function generator, power amplifier, power meter 1, power meter 2, digital multimeter, multimeter, thermocouple, prototype ohmic treatment chamber, software, and the material used is honey.

C. Research Variables

This study involves several main variables summarized in Table 1 below:

Table 1. Research Variables

No	Variable	Value/Range/Parameter
	Frequency	50 Hz, 300 Hz, 1 kHz, 3 kHz
2.	Temperature	63°C
3.	Duration	30 minutes
4.	Evaluation Metrics	MSE, PSNR, SSIM, FSIM, and Entropy

D. Research Object

The object of this study is aluminum electrodes, which serve as the main component in ohmic heating systems. The selection of aluminum electrodes is based on their high electrical conductivity and relevance in various electrochemical applications.

E. Experimental Conditions

Aluminum electrodes were mounted in an ohmic heating chamber containing honey samples. The heating process was conducted at a constant voltage of 300 VAC and a temperature of 63°C for 30 minutes at each frequency. Voltage and temperature conditions were controlled using a power meter and thermocouple. Additionally, each treatment was repeated at least twice to ensure reproducibility of results.

F. Image Acquisition Conditions

Electrode images were obtained using a HAYEAR 4K digital microscope with a maximum resolution of 1920 × 1080 pixels. Image acquisition was performed by optimizing the LED lighting intensity ( ) to achieve uniform illumination, with the camera positioned 10 cm from the object. Additionally, images were obtained under two different conditions: before and after ohmic heating.

G. Image Acquisition Flowchart

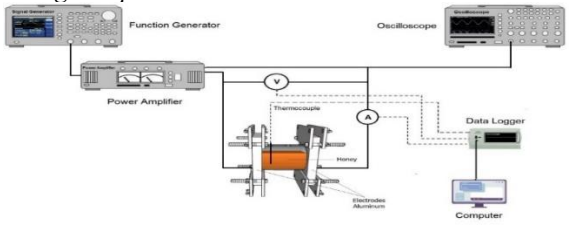

Fig. 6 Schematic Diagram of the Ohmic Heating Extraction System

Based on the schematic diagram of the ohmic heating and image acquisition process, the system consists of:

1. Function Generator: Generates an electrical signal with a specific frequency and waveform as the initial power source for ohmic heating.
2. Power Amplifier: Amplifies the signal from the generator to ensure the electrical current is strong enough to heat the honey.
3. The honey sample is placed between two aluminum electrodes in the ohmic heating chamber, with a clamping system to maintain optimal contact.
4. Measuring Instruments
   - *Voltmeter* (V): Measures the electrical voltage applied to the sample.
   - Ammeter (A): Measures the electric current flowing through the honey sample
   - *Thermocouple*: A sensor for monitoring the temperature of the honey sample during the heating process.
5. Oscilloscope: Used to visualize and analyze the electrical signals generated during the heating process.
6. Data Logger: During the extraction process, this device records all current, voltage, and temperature measurements in real-time.
7. Computer: Connected to the data logger to acquire, manage, and review the collected data.

H. Interpretation of Quality Metrics for Image Evaluation in the Detection of Microstructural Damage in Electrodes

In this study, edge detection results using the hybrid Canny-Sobel and Holistically-Nested Edge Detection (HED) methods were quantitatively evaluated using several image quality metrics, namely MSE, PSNR, SSIM, FSIM, and Entropy. The interpretation of each metric in the context of microstructure damage detection on aluminum electrodes is as follows:

1. MSE: A high MSE value indicates significant damage to the electrode, while a low value indicates minimal changes and a stable surface.
2. PSNR: High PSNR values indicate good image quality and minimal damage, while low PSNR values indicate significant damage to the electrodes.
3. SSIM: A SSIM value close to 1 indicates an intact electrode structure, while a low value indicates damage or corrosion.
4. FSIM: High FSIM indicates well-preserved electrode details, while low values indicate damage.
5. Entropy: High entropy indicates damaged electrode surfaces, while low entropy indicates better-preserved surfaces.

I. Result Validation Procedure

The validation process of the results in this study was conducted in two main stages as follows:

1. Edge detection was compared visually and quantitatively with reference images of the electrode before and after heating. Visual validation assessed edge brightness and sharpness, while quantitative evaluation used MSE, PSNR, SSIM, FSIM, and Entropy to measure the accuracy and consistency of the results.
2. The second stage involves matching the image analysis results with metal contamination tests using ICP-OES to ensure that electrode damage detection reflects its impact on honey quality.

J. Research Stages

The implementation of this research was carried out through several organized and systematic stages as shown in the following flowchart:

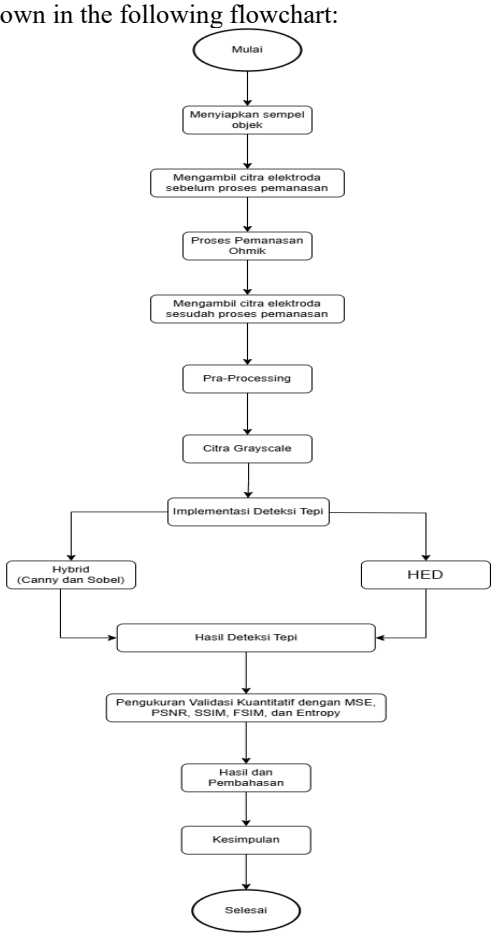

Fig. 7 Flowchart of Research Stages

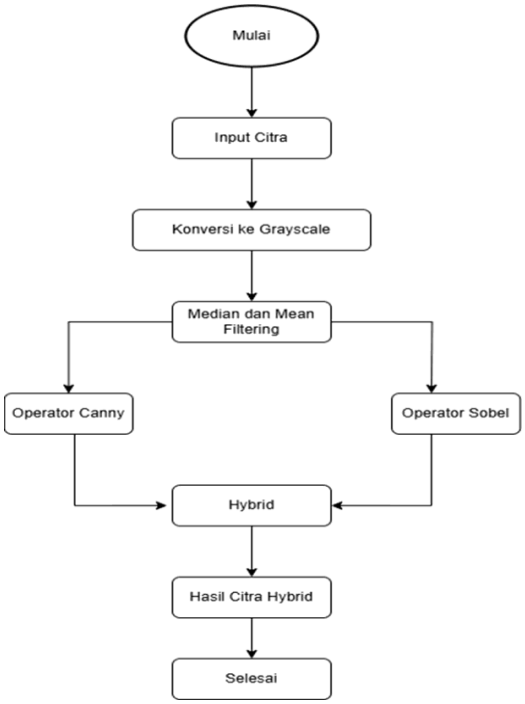

Fig. 8 Edge Detection Process using the Hybrid Method

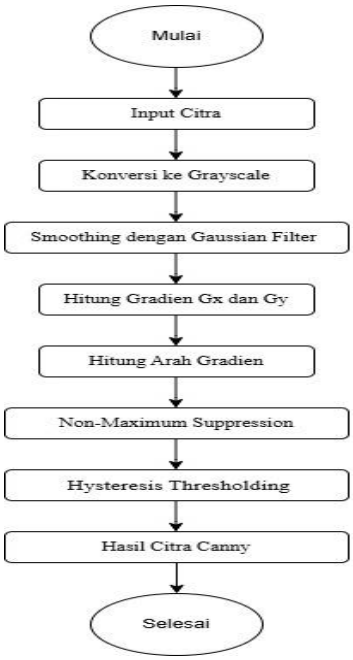

Fig. 9 Edge Detection Process using the Carry Method

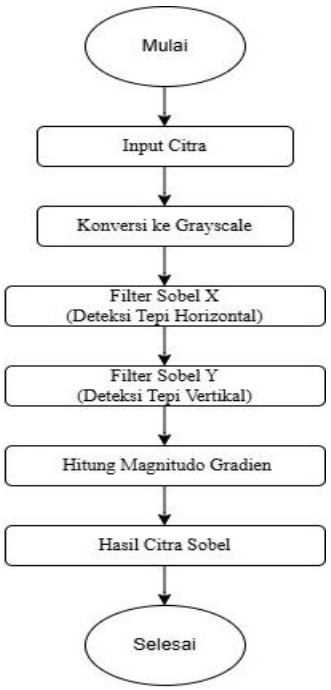

Fig. 10 Edge Detection Process using the Sobel Method

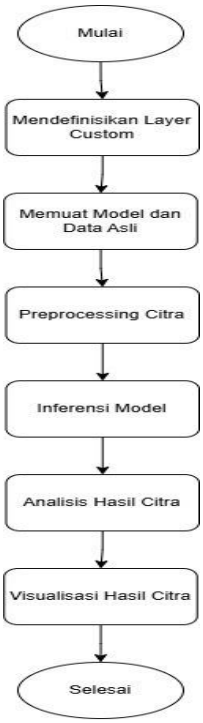

Fig. 11 Edge Detection Process Using the HED Method

This study systematically selected the Canny-Sobel hybrid method and Holistically-Nested Edge Detection (HED) to detect the edges of aluminum electrode microstructures. Canny-Sobel was chosen for its speed and efficiency, while HED was used to achieve more detailed and accurate detection through a deep learning approach. Analysis was conducted on electrode images before and after ohmic heating with frequency-varying , using

evaluation metrics such as MSE, PSNR, SSIM, FSIM, and Entropy.

In addition to image analysis, edge detection results were verified using laboratory test data on metal contamination levels in honey via ICP-OES. This approach supports the research objectives of evaluating electrode damage non-destructively, comparing the effectiveness of two edge detection methods, and developing an efficient electrode quality monitoring system for food industry applications.

IV. RESULTS AND DISCUSSION

A. Edge Detection Results

A.1 Hybrid Canny and Sobel Edge Detection Results

The implementation of the hybrid method on the study dataset produced edge detection images displayed in the following table:

Table 2. Hybrid Canny and Sobel Edge Detection Results

Frequency	Electrode	Before	After
50 Hz	Right	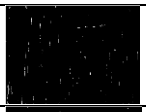	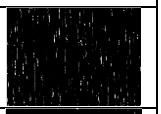
	Left	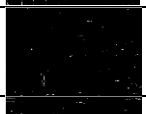	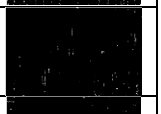
300 Hz	Right		
	Left	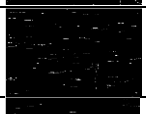	
1 kHz	Right	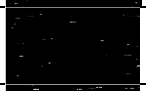	
	Left	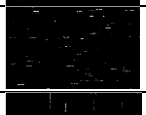	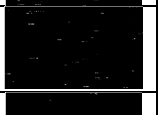
3 kHz	Right	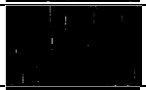	
	Left		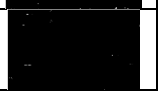

The results of edge detection analysis using the Canny-Sobel hybrid approach show significant structural changes in the electrodes after heating, particularly at a frequency of 50 Hz, where the edges appear sharp and clear due to high electrochemical activity. As the frequency increases, the intensity of edge detection decreases; at 300 Hz, the edge pattern becomes more dispersed, while at 1 kHz, the structure appears more stable. Optimal conditions are achieved at 3 kHz, with minimal changes, indicating low electrochemical interaction and better structural stability.

A.2 Results of Holistically-Nested Edge Detection (HED)

The results of implementing the Holistically-Nested Edge Detection (HED) method on the research dataset are presented in the following table:

Table 3. HED Edge Detection Results

Frequency	Electrode	Before	After
50 Hz	Right		
	Left		
300 Hz	Right	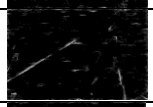	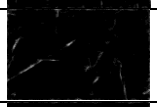
	Left	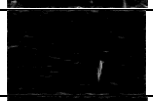	
1 kHz	Right		
	Left		
3 kHz	Right		
	Left		

Based on the edge detection results using the Holistically-Nested Edge Detection (HED) method, significant differences were observed in the surface structure of the electrode before and after ohmic heating, particularly at the low frequency of 50 Hz, indicating high electrochemical reactions and corrosion potential. At a frequency of 300 Hz, the intensity of the edge lines begins to decrease, indicating a reduction in electrochemical reactions. Meanwhile, at a frequency of 1 kHz, the edge pattern appears more minimal, indicating fewer structural changes. Overall, high frequencies have proven effective in reducing electrochemical reactions and the risk of metal contamination in food.

B. Image Quality Evaluation Using Quantitative Metrics

Quantitative analysis of images obtained from hybrid edge detection and Holistically-Nested Edge Detection (HED) was conducted using five complementary image quality metrics to provide an objective evaluation of algorithm performance.

B.1 Calculation Results of Hybrid Method Metric Values

The results of metric value calculations for various frequencies and *hybrid* edge detection methods combining the Canny and Sobel methods are presented in Table 4. As follows:

Table 4. Metric Evaluation Results for Aluminum Electrode Images

Metode	Gambar	Frekuensi	MSE	PSNR (Db)	SSIM	FSIM	Entropy	ICP-OES mg/kg
Hybrid	Before kanan	50Hz	1024.502	18.026	0.954	0.016	0.294	89,35
	Before kiri		927.212	18.459	0.968	0.028	0.233	
	After kanan		1938.893	15.255	0.880	0.000	0.601	
	After kiri		1092.008	17.749	0.960	0.025	0.274	
	Before kanan	300Hz	1362.938	16.786	0.936	0.067	0.391	70,6
	Before kiri		1368.307	16.769	0.933	0.011	0.404	
	After kanan		1107.243	17.688	0.959	0.081	0.283	
	After kiri		1050.592	17.916	0.964	0.019	0.266	
	Before kanan	1Khz	1004.975	18.109	0.967	0.004	0.245	30.79
	Before kiri		1166.225	17.463	0.945	0.001	0.344	
	After kanan		1002.053	18.122	0.967	0.000	0.244	
	After kiri		910.413	18.538	0.969	0.000	0.232	
	Before kanan	3Khz	986.238	18.191	0.969	0.003	0.235	ND(<0,03)
	Before kiri		900.306	18.587	0.977	0.003	0.198	
	After kanan		932.210	18.436	0.975	0.021	0.206	
	After kiri		892.203	18.626	0.978	0.000	0.195	

Based on Table 4, the metric evaluation of aluminum electrode images using the Holistically-Nested Edge Detection (HED) method shows significant differences depending on the heating frequency. The best conditions were detected on the left electrode at a frequency of 3 kHz, yielding an MSE of 108.557, PSNR of 27.774 dB, SSIM of 0.824, FSIM of 0.001, and Entropy of 2.282, indicating accurate edge detection with low noise and preserved structure. At a frequency of 1 kHz, performance remained stable with a higher SSIM despite an increase in MSE. The image of the right electrode at 300 Hz also showed good quality, while the frequency of 50 Hz on the left electrode exhibited the highest degradation, though the results were still acceptable.

Laboratory tests using ICP-OES confirmed the correlation between heating frequency and aluminum contamination in honey. At the low frequency of 50 Hz, aluminum contamination reached 89.35 mg/kg, indicating high corrosion due to intense electrochemical activity. Increasing the frequency to 300 Hz reduced contamination to 70.6 mg/kg, and further decreased to 30.79 mg/kg at 1 kHz. A frequency of 3 kHz yielded the best results with undetectable contamination (0.03 mg/kg), indicating that high-frequency ohmic heating is highly effective in maintaining electrode integrity and preventing product contamination.

a. Combined MSE and PSNR Graph

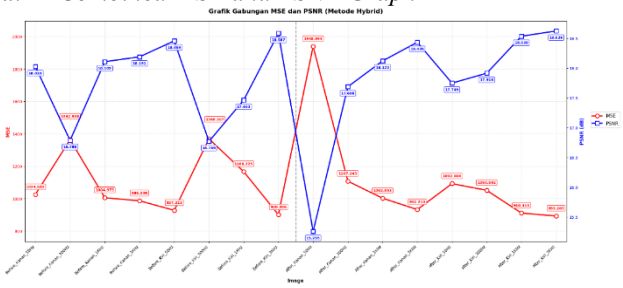

Fig. 12 Combined MSE and PSNR Graph

Fig. 12 shows the image quality assessment using MSE and PSNR. The highest MSE value occurred at After Right 50 Hz, while the lowest was at After Left 3 kHz, indicating the best reconstruction. Overall, the post-processing conditions resulted in lower MSE values, proving the effectiveness of the hybrid technique in improving image quality.

The graph shows an inverse correlation between MSE and PSNR, with the highest PSNR of 18.626 dB at After Left 3kHz and the lowest at 15.255 dB at After Right 50Hz. This pattern confirms the consistency of both metrics in evaluating image quality. The performance of the hybrid method is significantly influenced by the signal frequency used.

b. Combined SSIM, FSIM, and Entropy Graph

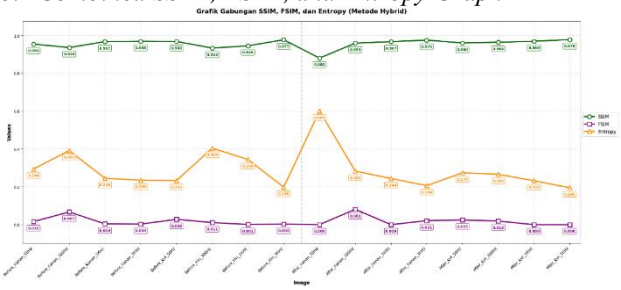

Fig. 13 SSIM, FSIM, and Entropy Graph

Fig. 13 shows high SSIM values (0.880–0.978), indicating that the hybrid method effectively preserves the electrode image structure. The decrease in SSIM at After Right 50Hz confirms the poorest quality, as indicated by MSE and PSNR. Overall, this method successfully maintains important image details well.

The very low FSIM values (0.000–0.083) indicate potential issues in estimation or mismatch between the image and the algorithm. Entropy varies (0.190–0.601), with the highest value at After Right 50Hz, indicating high complexity and noise. This variation reflects that the hybrid method produces different image quality depending on the input conditions.

B.2 Metric Value Calculation Results for the Method (HED)

The results of metric value calculations for various frequencies and edge detection methods using *Holistically-Nested Edge Detection* (HED) are presented in Table 5 below:

Table 5. Metric Evaluation Results for Aluminum Electrode Images

Method	Image	Frequency	MSE	PSNR	SSIM	FSIM	Entropy	ICP-OES mg/kg
HED	Before kiri	50Hz	352.978	22.653	0.559	0.016	3.794	89,35
	Before kanan		357.381	22.597	0.652	0.015	3.543	
	After kiri		265.103	23.897	0.707	0.011	3.088	
	After kanan		311.922	23.190	0.687	0.001	3.236	
	Before kiri	300Hz	178.287	25.620	0.723	0.008	3.025	70,6
	Before kanan		577.979	20.512	0.431	0.020	4.693	
	After kiri		151.838	26.317	0.804	0.009	2.472	
	After kanan		301.562	23.337	0.712	0.018	3.160	
	Before kiri	1Khz	183.358	25.498	0.842	0.003	2.105	30.79
	Before kanan		155.377	20.512	0.822	0.001	2.250	
	After kiri		143.052	26.317	0.841	0.001	2.040	
	After kanan		119.421	23.337	0.817	0.001	2.236	
	Before kiri	3Khz	575.062	28.859	0.826	0.004	2.243	ND(<=0,03)
	Before kanan		562.000	20.633	0.547	0.004	4.179	
	After kiri		108.557	27.774	0.824	0.001	2.282	
	After kanan		401.016	22.089	0.490	0.001	4.372	

Based on Table 5, the metric evaluation results of aluminum electrode images using the Holistically-Nested Edge Detection (HED) method indicate that detection capability is significantly influenced by heating frequency. At 3 kHz, the best results were obtained on the left electrode, with a low MSE (108.557), high PSNR (27.774 dB), and stable SSIM and Entropy values, indicating optimal image sharpness and stability. At a frequency of 1 kHz, performance remains good with consistent metric values, indicating detection stability. The right electrode image at a frequency of 300 Hz also shows very good image quality, while the frequency of 50 Hz shows the highest degradation, although still within acceptable limits.

Laboratory tests using the ICP-OES method showed a correlation between ohmic heating frequency and aluminum contamination levels in honey. The low frequency of 50 Hz showed the highest contamination at 89.35 mg/kg due to high electrochemical activity. When the frequency was increased to 300 Hz and 1 kHz, contamination decreased drastically to 70.6 mg/kg and 30.79 mg/kg. The most optimal results were observed at a frequency of 3 kHz, where metal contamination was not detected (<0.03 mg/kg), indicating that high-frequency heating effectively reduces electrode damage and maintains honey quality from metal contamination.

a. Combined MSE and PSNR Graph

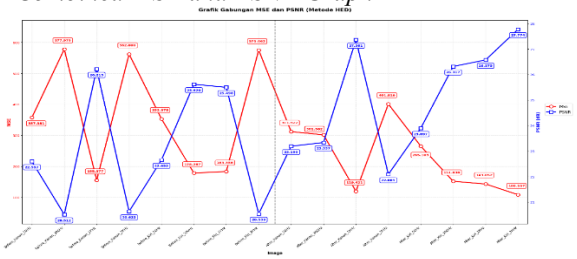

Fig. 14 Combined MSE and PSNR Graph

Fig. 14 shows a negative correlation between MSE and PSNR, where high MSE results in low PSNR, and vice versa. The best example is After Left 3kHz with the lowest MSE and highest PSNR, indicating the best image reconstruction quality. This proves that HED performance is influenced by noise and image frequency.

b. Combined SSIM, FSIM, and Entropy Graph

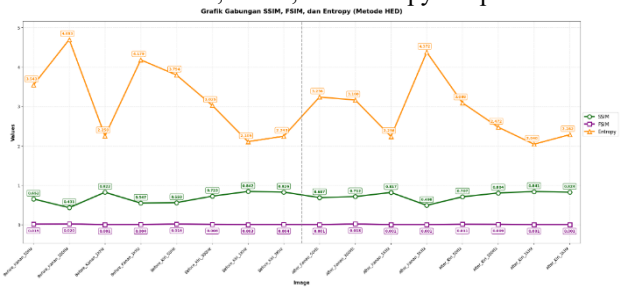

Fig.15 SSIM, FSIM, and Entropy Graph

Fig. 15 shows that the HED method is capable of preserving image structure and features with stable SSIM and FSIM values. Variations in entropy values indicate HED's ability to reduce noise while maintaining important image information.

Analysis shows that HED is more effective at high frequencies, with PSNR increasing and MSE decreasing, proving its ability to preserve image details during processing.

C. HED Analysis Superior in Theoretical Aspects

Theoretically, Holistically Nested Edge Detection (HED) outperforms conventional methods such as Canny and Sobel because it uses a deep learning architecture based on CNN that can extract features at various scales. HED integrates information from various levels of network depth, enabling the detection of fine details and complex microstructural patterns on electrode surfaces. Its ability to adapt to noise and texture variations makes HED more accurate and consistent in detecting microstructural damage caused by ohmic heating.

V. CONCLUSION AND RECOMMENDATIONS

A. Conclusion

- The evaluation shows that low frequencies, such as 50 Hz, cause the most significant electrode damage with aluminum contamination reaching 89.35 mg/kg. Contamination decreases with increasing frequency: 70.6 mg/kg at 300 Hz, 30.79 mg/kg at 1 kHz, and undetectable (<0.03 mg/kg) at 3 kHz. This proves that high frequencies effectively reduce electrochemical reactions and electrode damage.
- The HED method outperforms the hybrid Canny-Sobel method as it can non-destructively detect fine details of microstructural damage.
- The HED method yields the best results at a frequency of 3 kHz for the left electrode, with an MSE of 108.557, PSNR of 27.774 dB, SSIM of 0.824, FSIM of 0.001, and Entropy of 2.282. These values reflect accurate edge detection and accurately represent the electrode damage conditions.
- Both methods are effective, but HED is more recommended for digital monitoring due to its more detailed and precise results.

B. Recommendations

- Further research is needed to expand the image dataset and evaluate different conditions such as temperature, humidity, voltage, duration, and electrode type to gain a deeper understanding of the damage mechanism.
- It is recommended to develop a deep learning-based edge detection method for real-time monitoring systems to enhance the efficiency and safety of ohmic heating in the food industry.
- Electrode microstructure analysis should be complemented with SEM and digital imaging methods for more detailed and accurate results regarding electrode damage.

REFERENCES

[1] Annatasia, K., Sitepu, B., and Hanafiah, M.A. (2023) 'Combination of Prewitt and Canny Edge Detection Algorithms for Identifying Inverted Blood Type A+ Images', 5(1), pp. 132–140. Available at: https://tunasbangsa.ac.id/pkm/index.php/brahmana/article/view/286.

[2] Asmaidi, A. *et al.* (2019) 'Implementation of Sobel Method Based Edge Detection for Flower Image Segmentation', *SinkrOn*, 3(2), p. 161. Available at: https://doi.org/10.33395/sinkron.v3i2.10050.

[3] Evahelda, E., Pratama, F., and Santoso, B. (2017) 'Physical and Chemical Properties of Honey from Rubber Tree Nectar in Bangka Tengah Regency, Indonesia', *Agritech*, 37(4), p. 363. Available at: https://doi.org/10.22146/agritech.16424.

[4] Hartono, E.D. *et al.* (2024) 'Characterisation of honey using high-frequency ohmic heating based on image segmentation', pp. 1–11. Available at: t: https://doi.org/https://doi.org/10.21776/ub.afssaae.2024.007.03.8.

[5] Hartono, E. D., *et al.* (2025). 'Prediction Analysis of Heat Penetration in Ohmic Heating using Multivariate Long Short-Term Memory Networks', Engineering, Technology & Applied Science Research, 15(3), 22527–22537. https://doi.org/10.48084/etasr.10063

[6] Herawati, D. and Kardian, A.R. (2018) 'Edge Detection Analysis on JPG-Based Digital Images Using the Canny Operator with Matrix Laboratory', *Journal of Computational Science*, 17(3), pp. 191–208. Available at: https://ejournal.jak-stik.ac.id/index.php/komputasi/article/view/2414.

[7] Herlambang, A. and Rahmatulloh, A. (2025) 'Improving Edge Detection Accuracy in Inverse Images Using Sobel-Canny-Prewitt', *Journal of Informatics and Multimedia*, 17(1), pp. 38–45. Available at: https://doi.org/10.33795/jtim.v17i1.6590.

[8] Hutasoit, J.P., Ermayana, R.A., and Sutrisno, A. (2023) 'The Effect of Voltage Variation in the Ohmic Heating Pasteurization Process on the Characteristics of Wild Horse Milk from Sumbawa', *Journal of TAMBORA*, 7(2), pp. 38–44. Available at: https://doi.org/10.36761/jt.v7i2.2984.

[9] Kurniawan, T.R. and Pamungkas, D.P. (2024) 'Segmentation of Red Onion Leaf Images Using the Canny Edge Detection Method', 07(01), pp. 82–87. Available at: https://doi.org/https://doi.org/10.29407/noe.v7i01.20558.

[10] Kurniawati, I.D. and Kusumawardhani, A. (2017) 'Implementation of the Canny Algorithm in Face Recognition Using the Matlab GUI Interface', *Journal of the Institute of Technology Ten November*, (December), pp. 3–8. Available at: https://www.researchgate.net/publication/321747638_Implementasi_Algoritma_Canny_dalam_Pengenalan_Wajah_Menggunakan_Antarmuka_GUI_Matlab.

[11] Maximillian, L. *et al.* (2023) 'Comparison of Sobel and Canny Algorithms for Edge Detection in Aloe Vera Leaf Images', *Komputa: Journal of Computer Science and Informatics*, 12(2), pp. 69–79. Available at: https://doi.org/10.34010/komputa.v12i2.10997.

[12] Mercali, G.D. *et al.* (2013) 'Degradation kinetics of anthocyanins in acerola pulp: Comparison between ohmic and conventional heat treatment', *Food Chemistry*, 136(2), pp. 853–857. Available at: https://doi.org/10.1016/j.foodchem.2012.08.024.

[13] Munantri, N.Z., Sofyan, H., and Florestiyanto, M.Y. (2020) 'Application of Digital Image Processing for Tree Age Identification', *Telematika*, 16(2), p. 97. Available at: https://doi.org/10.31315/telematika.v16i2.3183.

[14] Mustafid, A. and 'Uyun, S. (2017) 'Segmentation of Cattle Images Based on Edge Detection Using the Canny Edge Detection Algorithm', *Jurnal Buana Informatika*, 8(1), pp. 27–36. Available at: https://doi.org/10.24002/jbi.v8i1.1074.

[15] Noviana, L.P.R., Indrawan, I.P.E., and Setiawan, G.I. (2024) 'ANALYSIS OF CANNY EDGE DETECTION METHOD FOR FACIAL RECOGNITION IN DIGITAL IMAGE PROCESSING', *Journal of Management and Information Technology (JMTI)*, pp. 1–6. Available at: https://doi.org/https://doi.org/10.59819/jmti.v15i2.4107.

[16] Rajuddin, M. *et al.* (2024) 'Disease Detection System on Mango Leaves Using Sobel and Canny Edge Detection Methods', pp. 1–7. Available at: https://proceedings.unimal.ac.id/senastika/article/view/872.

[17] Sumarlin, L.O. *et al.* (2022) 'Characteristics and Antibacterial Activity of Apis and Trigona Honey Types against Escherichia coli and Staphylococcus Aureus on Various Heating', *Journal of Valency Chemistry*, 8(2), pp. 251–262. Available at: https://doi.org/10.15408/jkv.v8i2.27241.

[18] Syamsul, T.D., Lala, and Syaharuddin (2022) 'Phytochemical Content, Polyphenols, and Flavonoids in Trigona Honey (Tetragonula biroi) from Bone, South Sulawesi', *Journal of Training and Community Service Adpertisi (JTCSA)*, 2(2), pp. 62–70. Available at: https://jurnal.adpertisi.or.id/index.php/JTCSA/article/view/424.

[19] Wibowo, S.A. *et al.* (2021) 'Performance of Pasteurization Equipment in the Pasteurization of Honey: A Case Study of PT Kembang Joyo Sriwijaya', *Journal of Agricultural Engineering and Biosystems*, 9(1), pp. 11–21. Available at: https://doi.org/10.29303/jrpb.v9i1.181.

[20] Wulandari, M. (2017) 'Quality assessment index of interpolated images (SSIM and FSIM)', *Journal of Applied Information Technology*, pp. 11–20. Available at: https://doi.org/https://doi.org/10.21460/jutei.2017.11.5.

[21] Xie, S. and Tu, Z. (2015) 'Holistically-Nested Edge Detection', pp. 1–9. Available at: https://doi.org/https://doi.org/10.1109/ICCV.2015.16.